

1 **ABSTRACT**

2 Mixing regime and CO<sub>2</sub> availability may control cyanobacterial blooms in polymictic lakes, but  
3 the underlying mechanisms still remain unclear. We integrated detailed results from a natural  
4 experiment comprising an average-wet year (2011) and one with heat waves (2012), a long-term  
5 meteorological dataset (1960–2010), historical phosphorus concentrations and sedimentary  
6 pigment records, to determine the mechanistic controls of cyanobacterial blooms in a eutrophic  
7 polymictic lake. Intense warming in 2012 was associated with: 1) increased stability of the water  
8 column with buoyancy frequencies exceeding 40 cph at the surface, 2) high phytoplankton  
9 biomass in spring (up to 125 mg WW L<sup>-1</sup>), 3) reduced downward transport of heat and 4)  
10 depleted epilimnetic CO<sub>2</sub> concentrations. CO<sub>2</sub> depletion was maintained by intense uptake by  
11 phytoplankton (influx up to 30 mmol m<sup>-2</sup> d<sup>-1</sup>) in combination with reduced, internal and external,  
12 carbon inputs during dry, stratified periods. These synergistic effects triggered bloom of buoyant  
13 cyanobacteria (up to 300 mg WW L<sup>-1</sup>) in the hot year. Complementary evidence from  
14 polynomial regression modelling using historical data and pigment record revealed that warming  
15 explains 78% of the observed trends in cyanobacterial biomass, whereas historical phosphorus  
16 concentration only 10% thereof. Together the results from the natural experiment and the long-  
17 term record indicate that effects of hotter and drier climate are likely to increase water column  
18 stratification and decrease CO<sub>2</sub> availability in eutrophic polymictic lakes. This combination will  
19 catalyze blooms of buoyant cyanobacteria.

20

21 Keywords: harmful blooms, carbon dioxide, climate warming, eutrophication, buoyant  
22 cyanobacteria.

## 23 **1 INTRODUCTION**

24 Harmful cyanobacterial blooms are of increasing concern globally, raising questions about the  
25 controls on their development (Ho & Michalak, 2015). Increasing surface air temperatures, the  
26 immediate consequence of climate change, reduce the duration of ice cover and, with a longer  
27 and warmer season, lake surface temperature and stratification also increase (Dibike et al.2011).  
28 In eutrophic lakes, such conditions stimulate phytoplankton growth and harmful blooms  
29 (Kraemer et al., 2017). Buoyant, bloom-forming cyanobacteria, for example, have an ecological  
30 advantage during warm stratified periods because they are capable to quickly optimize their  
31 vertical position in the water column (Ganf & Oliver, 1982). Indirect effects of climate change,  
32 such as altered precipitation patterns, catchment hydrology and reduced winds (Karnauskas et  
33 al., 2018), can also influence phytoplankton and favour cyanobacteria through effects on water  
34 clarity, retention times and mixing (Reichwaldt & Ghadouani, 2012).

35

36 It is well established that changes in nutrient concentration and stoichiometry, for  
37 example decreasing nitrogen (N) to phosphorus (P) ratios, can shift phytoplankton communities  
38 toward a greater contribution from cyanobacteria (Paerl et al., 2011). Numerous examples  
39 indicate that N limitation in stratified lakes may favour diazotrophic cyanobacteria (e.g., Gobler  
40 et al., 2016). With respect to carbon (C), cyanobacteria that are capable of efficiently exploit  
41 bicarbonates can also use CO<sub>2</sub> at lower concentrations than other phytoplankton species (Ibelings  
42 & Maberly, 1998; Posch et al., 2012) particularly when alkalinity is high (Caraco & Miller,  
43 1998). Buoyant cyanobacteria can also actively move to the air-water interface to efficiently  
44 exploit atmospheric CO<sub>2</sub>. Combined and interlinked effects of enhanced stratification and  
45 changes in nutrient ratios have led to the proliferation of cyanobacteria in stratified lakes globally  
46 (de Senerpont-Domis et al., 2007). There is, however, relatively little mechanistic understanding

47 of how these interacting factors impact cyanobacteria in nutrient-rich polymictic lakes (Kosten et  
48 al., 2012), where the water column mixes on a daily to weekly basis, and where the impacts of  
49 future climate, with changes in both temperature and rainfall, could affect physico-chemical  
50 conditions in potentially different ways.

51

52         Across the globe heat waves have become increasingly frequent as a consequence of  
53 climate change (Karl & Trenberth, 2003). The short-term responses of lakes to these events may  
54 provide specific insights into the longer-term effects of climate warming on the functioning of  
55 lake ecosystems (Havens et al., 2016). In polymictic lakes, strong stratification may develop  
56 during years with heat waves (Bartosiewicz et al., 2015). Periods of exceptionally hot weather  
57 can be interrupted by windy and/or rainy days when relatively deep mixing and/or high runoff  
58 supplies pulses of nutrients and carbon to lakes. Buoyant cyanobacteria may benefit from  
59 stratification and intermittent mixing by making the most efficient use of the unsteady supply of  
60 resources (Huber et al., 2012). Correlative evidence indicates that the combined effects of  
61 warmer temperatures, thermal stratification and nutrient loading can modulate the abundance of  
62 cyanobacteria in shallow lakes, but the interactive mechanisms behind these effects remain  
63 unclear (Kosten et al., 2012).

64

65         Natural experiments comparing average and heat-wave years (e.g., Jankowski et al.,  
66 2006; Bartosiewicz et al., 2016) provide qualitative constraints on the potential links between  
67 climatic effects and the proliferation of cyanobacteria in lakes (Jöhnk et al., 2008). However, the  
68 integration of studies spanning interannual to interdecadal timescales and using multiple proxies  
69 provides more robust information on potential mechanisms. Recent survey of sedimentary  
70 pigment records and meteorological data for 83 lakes shows that cyanobacterial abundance is

71 controlled by nutrient and temperature effects, with the former explaining three times more of  
72 the observed variation than the latter (Tarnau et al., 2015). However, among the 83 lakes taken  
73 into consideration, only a few were shallow (6 lakes < 9 m deep). The functioning of shallow,  
74 polymictic lakes differs greatly from larger and deeper water bodies, and thus further  
75 investigation is required to determine the global applicability of these relationships. In this  
76 context, it is important to underline that small and shallow lakes represent approximately half of  
77 the global lentic area (Verpoorter et al., 2014), and that the impact of warming air temperatures  
78 on the physical structure and phytoplankton of these ecosystems may be more immediate than in  
79 larger and deeper lakes.

80

81 This study aimed to provide insight into the synergistic effects of limnological conditions  
82 related to atmospheric warming, including reduced precipitation, enhanced water column  
83 stability, increased surface-water temperature and CO<sub>2</sub> depletion, which together catalyze  
84 cyanobacterial blooms. This was done by: 1) comparing measures of stratification, nutrient  
85 regimes, CO<sub>2</sub> concentrations, and phytoplankton community in a shallow eutrophic, polymictic  
86 lake over two years, one of which presented heat-wave conditions; and 2) integrating records of  
87 sedimentary pigments with meteorological data and historical P and CO<sub>2</sub> concentrations.

88

## 89 **2 METHODS**

### 90 **2.1 Study site and regional climate**

91 Lake St. Augustin (46° 42'N, 71° 22'W) is a small (0.63 km<sup>2</sup>) and shallow (average depth of 3.5  
92 m) lake located on the outskirts of Quebec City (Figure 1). In the past two centuries, the lake has  
93 been exposed to the effects of intensified farming and urbanization (Deshpande et al., 2014) and  
94 became eutrophic by the mid-twentieth century. Currently, the lake is still classified as eutrophic

95 to hypereutrophic, with total phosphorus concentrations (TP) between 20-160  $\mu\text{g L}^{-1}$  and  
96 summertime chlorophyll-a (Chl-a) concentrations between 20 and 60  $\mu\text{g L}^{-1}$ .

97

## 98 **2.2 Interannual meteorology and physicochemistry**

99 In 2011 and 2012, the lake was sampled at bi-weekly to monthly intervals throughout the entire  
100 open-water season (3 May – 13 October 2011, 22 April – 18 October 2012). During these two  
101 years, meteorological data were obtained from an Environment Canada weather station located  
102 1.5 km from the lake (<http://climate.weather.gc.ca/>).

103

104 Water column profiles of temperature, conductivity, pH and dissolved oxygen (DO) were  
105 measured with a 600R multi-parametric probe (Yellow Spring Instruments). In addition, a  
106 thermistor chain (Onset Tidbit v2; accuracy 0.2°C, resolution 0.2°C, response time of 5 min) was  
107 installed to measure water temperature from June to October 2012 in the pelagic zone of the lake  
108 (10 m inshore from the regular sampling station, Figure 1), with loggers deployed at 10 depths  
109 (0, 0.2, 0.4, 0.8, 1.2, 2.0, 2.5, 3.0, 3.5 and 4.0 m), and recording at 4-minute intervals. The  
110 dynamics of the diurnal mixed layer were evaluated using equations developed by Imberger  
111 (1985), and the surface energy budget was computed following MacIntyre et al. (2002). We  
112 computed buoyancy frequency  $N = (g/\rho \, d\rho/dz)^{1/2}$  where  $g$  is gravity,  $\rho$  is density, and  $z$  is depth.  
113 Salinity ( $S$ ) was computed as a function of specific lake water conductance ( $550\text{-}650 \mu\text{S cm}^{-1}$ ),  
114 by multiplying by a factor 0.8, as an estimate for the typical range between 0.6 and 0.9  
115 (Pawlowicz 2008). Density was computed from temperature and salinity of  $0.48 \text{ g kg}^{-1}$  (Chen &  
116 Millero, 1977; MacIntyre, et al., 2018). As meteorological data were not collected on site, we  
117 computed a heat budget for the lake based on measured temperatures and bathymetric data and  
118 compared it with that obtained from the meteorological data. We sequentially reduced winds

119 until the two budgets matched, and obtained congruence for wind speeds that were 70% of those  
120 recorded at the weather station. Lake number ( $L_N$ ) was computed following Imberger and  
121 Patterson (1990) using the reduced wind speeds.

122

123 On each sampling date, discrete surface and near-bottom water samples taken at the  
124 deepest point of the lake were filtered through cellulose acetate filters (0.2- $\mu\text{m}$  pore size) for the  
125 analyses of soluble reactive phosphorus (SRP, duplicates, detection limit, DL, of 0.5  $\mu\text{g L}^{-1}$ ) and  
126 nitrogen ( $\text{N-NO}_3^-$ , DL of 0.01  $\text{mg L}^{-1}$ ) using standard methods (Stainton et al., 1977). Total  
127 phosphorus and nitrogen analyses were carried out on unfiltered water samples following  
128 Stainton et al. (1977). Surface-water samples (100–500 ml, in duplicates) were also filtered  
129 through GF/F glass fiber filters (0.7- $\mu\text{m}$  pore size) for the determination of Chl-*a* concentration  
130 by UV–Vis spectrophotometry after extraction of pigments in ethanol (Winterman & De Mots,  
131 1965). The  $\text{CO}_2$  concentrations (in triplicates) were assessed by equilibrating 2.0 L of water with  
132 20 ml of air. After equilibration, the headspace was sampled into He-purged, pre-evacuated  
133 Exetainers (Labco Limited, UK), and the collected gas was analyzed as described in Laurion et  
134 al. (2010). The  $\text{CO}_2$  fluxes were measured with a floating chamber (circular, 23.4 L), made of 10  
135 mm thick PVC plastic with floaters distributed evenly on the sidewall, extending 4 cm into the  
136 water, which was equipped with an infra-red gas analyzer (EGM-4, PP-Systems), and deployed 2  
137 m away from the boat during each sampling for up to 20 minutes during the day (10-14h) and  
138 every 6h over 24h period in July 2012.

139

### 140 **2.3 Phytoplankton**

141 For phytoplankton analyses, 1L water samples were collected from 0 to 5 meters at 1 m  
142 intervals, integrated by taking subsamples from each depth, preserved with Lugol's iodine

143 solution (5% final concentration) and analyzed following Utermohl (1958) using an inverted  
144 microscope (Zeiss Axiovert 2000). The threshold for defining bloom was taken at  $10^4$  cell per  
145 ml. The biovolumes were calculated following Hillebrand et al. (1999).

146

## 147 **2.4 Sedimentary pigments**

148 A single sediment core was retrieved in January 2011 using an open-barrel corer deployed at the  
149 deepest point of the lake, close to the main sampling station (Figure 1). The core was sub-  
150 sectioned at 0.5-cm intervals between 0 and 20 cm and sediment samples (6 to 7 g) were  
151 collected for pigment analysis were frozen and freeze-dried for 48 h, then stored at  $-20^{\circ}\text{C}$  until  
152 further processing. A description of the sediment lithology and a  $^{210}\text{Pb}$  and  $^{137}\text{Cs}$ -based age  
153 model, validated with  $^{14}\text{C}$  accelerator mass spectrometry (AMS) measurements, is provided in  
154 Deshpande et al. (2014). After extraction of approximately 0.2 g of dried sediment in 90%  
155 acetone and subsequent filtration of the extract, pigments were quantified by high performance  
156 liquid chromatography, and analyzed according to Zapata et al. (2000). All pigment  
157 concentrations are reported in *micrograms per gram of sediment organic matter* [ $\mu\text{g (g OM)}^{-1}$ ].  
158 Chlorophyll-a (Chl-a : Pheophytin  $>0.5$ ; Chl-a : Pyropheophytin  $>2.0$ ) and  $\beta$ -carotene (stable)  
159 were used as a general biomarkers of phytoplankton biomass, and zeaxanthin, echinenone and  
160 canthaxanthin as a quantitative proxy of cyanobacterial biomass (total cyanobacterial pigments).  
161 Zeaxanthin is also present in some rhodophytes and chlorophytes but in concentrations that are  
162 ten times lower than those reported for cyanobacteria (i.e., *Aphanizomenon gracile*, Schlüter et  
163 al. 2006). Furthermore, as blooms in Lake St-Agustin consist interchangeably of cyanobacteria,  
164 dinophytes or diatoms (Bouchard-Valentine, 2004), we considered that change in zeaxanthin is  
165 most likely associated with cyanobacterial biomass. A long-term ( $\sim 400$  years) pigment record

166 from this core was previously reported by Deshpande et al. (2014), while in the current study, we  
167 focused on the last 50 years (~1960 to 2010). This higher resolution data set (with 20 dates  
168 obtained over the 50-year period) was related to climate change indices and historical total  
169 phosphorus concentrations (TP). Data on past changes in TP for Lake St. Augustin were taken  
170 from various sources (available from <http://www.lacsaintaugustin.com/>), but all measurements  
171 were done using the same colorimetric method (Table S1). Past summertime CO<sub>2</sub> concentrations  
172 in surface waters were calculated using total alkalinity and pH values following approach by  
173 Millero et al. (2002). These data were available for 12 individual years between 1968 and 2010.

174

## 175 **2.5 Statistical analyses**

176 The data collected in 2011 and 2012 were compared using a Welch t-test (hereafter referred to as  
177 t-test), which accounts for unequal sampling frequency. For the polynomial regression analysis  
178 historical meteorological and P data were treated as independent and sedimentary pigment  
179 concentrations as depended variables. Temperatures (summer and winter) were averaged only for  
180 those years for which also sediment ages were available. For the analysis of snowfall versus  
181 sedimentary data, precipitation rates were averaged over the preceding winter. The historical  
182 phosphorus concentration (TP) record had lower temporal resolution than either the climate or  
183 sedimentary datasets, thus we limited the regression analysis only to years with available TP  
184 data. Correlations between sedimentary pigment concentrations, climatic conditions and  
185 phosphorus in Lake St. Augustin were also analyzed using sequential t-test followed by an  
186 ANOVA to reveal significant changes in temporal trends. The relationship between  
187 concentrations of specific pigments and P, surface air temperature and precipitation were

188 analyzed using a multiple polynomial regression model. All statistical analyses were performed  
189 with XLStat (2016).

190

### 191 **3 RESULTS**

#### 192 **3.1 Climate change and eutrophication in Lake Saint Augustin**

193 During the period covered by this study (1960 to 2010), the average air temperatures near  
194 the lake increased in winter and summer (Figure 2). The warming, however, was not linear. A  
195 sequential t-test followed by an ANOVA revealed a significant difference in warming trends  
196 between 1960-1990 and 1990-2010, with a faster increase during the latter period (Figure S1).  
197 Although there was no evident change in the overall amount of summertime rainfall, annual  
198 snowfall decreased significantly in the watershed of the lake during the last 50 years (Figure 2).

199

200 The first recorded TP concentrations from 1967 (values between 50 and 460  $\mu\text{g L}^{-1}$ ,  
201 average 220  $\mu\text{g L}^{-1}$ ) indicated severe phosphorus pollution. Later records indicate a decrease in  
202 TP to ca. 20  $\mu\text{g L}^{-1}$  between 1975 and 1983, an increase after 1983, and relatively high  
203 concentrations ( $> 25 \mu\text{g L}^{-1}$ ) persisting over the last three decades. These trends are well in range  
204 with previous estimates based on diatom fossils (Pienitz et al. 2006). No significant overall trend  
205 in the TP dataset was detected ( $p > 0.05$ ).

206

#### 207 **3.2 Meteorological conditions during an average and a heat-wave year**

208 The weather over Lake St. Augustin in May 2012 was hotter and drier in comparison to the  
209 previous year (Figure 3). For example, the average air temperature in May was in the upper 3%  
210 of the respective temperature distribution since 1945. Similarly, average temperatures in July and

211 August were in the upper 5% of respective distributions. In fact, the heat wave in August 2012  
212 made this month the warmest August in Quebec since 1945.

213

214 The average and maximum air temperatures for the summer were 16.2°C and 33°C in  
215 2012, respectively, as opposed to 15.3°C and 30°C in 2011 (Table 1). Rain events were less  
216 frequent during that period in 2012, and daily rainfall was lower than in 2011 (3.6 and 4.2 mm, t-  
217 test,  $p = 0.001$ ). Unusually long dry periods ( $> 7$  days) in July 2012 resulted in a low daily  
218 precipitation mean of 2.6 mm. The intensity of rain events was, however, greater in 2012 than in  
219 2011. Change in cumulative precipitation resulted in an increase of water retention time from  
220 188 days in 2011 to 223 days in 2012 (for calculation details see Bergeron et al., 2002).

221 Although in 2012, the average wind speed at the meteorological station was lower than in 2011  
222 (3.3 compared to 3.6  $\text{m s}^{-1}$ ), the frequency analysis did not reveal significant differences in  
223 energy on diurnal time scales (Figure 3).

224

### 225 **3.3 Stratification dynamics and biogeochemistry**

226 The surface waters in Lake St. Augustin were warmer in 2012 than in 2011 (21°C  
227 compared to 17°C,  $p = 0.05$ , t-test, Figure 4). In contrast, bottom waters remained colder during  
228 2012 (18°C compared to 19°C). Detailed temperature profiling revealed that the temperature  
229 difference between surface and bottom waters reached 9.5°C during the heat wave between 17  
230 and 21 June when air temperatures exceeded 30°C (Figure 4). The situation was similar during  
231 heat waves in July when temperature differences also regularly exceeded 5°C indicating strong  
232 stratification.

233 Temperatures exceeded 25°C in surface waters four times in the summer of 2012, times  
234 which corresponded to the heat waves (Figures 4 and 5). A critical component of the warming

235 was a decrease in wind speeds at night below the instrument threshold. Daytime winds varied  
236 during these periods, but were often less than  $4 \text{ m s}^{-1}$  and sometimes dropped to  $2 \text{ m s}^{-1}$ . These  
237 lower values contrast to winds speeds of up to  $6 \text{ m s}^{-1}$  when heat waves were not occurring. The  
238 Lake number ( $L_N$ ), an index of the extent of upwelling and downwelling of the thermocline, that  
239 is, the degree of tilting and the potential for mixing across it from breaking internal waves  
240 (Imberger & Patterson, 1990; MacIntyre et al., 2009), had values approaching 1 during daytime  
241 over these warm periods as opposed to values dropping an order of magnitude lower at other  
242 times (Figures 4 & 5). In response, the diurnal thermocline downwelled at the sampling site,  
243 which implies upwelling at the other end of the lake. The extent of downwelling was less during  
244 the warm periods (Figure 5). With the decrease in wind speeds at night and related increase in  
245  $L_N$ , the diurnal thermocline upwelled. Values of buoyancy frequency near the surface in the day  
246 were high enough during periods of heating to suppress near-surface mixing regardless of the  
247 mixing expected with low values of  $L_N$  (MacIntyre et al., 2018), and also increased in the lower  
248 water column during both day and night further indicating reduced mixing across the  
249 thermocline. Due to the low winds at night, and concomitantly decreased losses of heat by  
250 conduction and evaporation, nocturnal heat losses reached only up to  $-200 \text{ W m}^{-2}$ , as opposed to -  
251  $300 -500 \text{ W m}^{-2}$  on windier nights (data not shown). Hence, mixed layer deepening at night was  
252 suppressed (Figure 5, lower panel), much of the heat was retained, and stratification intensified.

253

254         During stormy conditions that started on 5 August 2012 (in the midst of a bloom),  
255 minimum values of  $L_N$  reached  $10^{-3}$ , which, if such conditions persisted, implies complete  
256 mixing (Figure 5) that would lead to changes in phytoplankton community. Indeed, the mixed  
257 layer did reach the lake bottom, but the lake re-stratified rapidly once the winds ceased. This  
258 rapid re-stratification implies that the water in the lower water column upwelled at the upwind

259 end of the lake, but full mixing did not occur. The estimates of turbulent mixing immediately  
260 below the mixing layer were of order  $10^{-6}$  to  $10^{-5} \text{ m}^2 \text{ s}^{-1}$ , indicating that mixing across the  
261 thermocline was not effective (Figure S2). Full water column mixing did occur, though,  
262 following a sustained event with low  $L_N$  at the beginning of September.

263

264 The biogeochemistry of the lake differed markedly between the two years, with the  
265 temperature and oxygen concentrations indicating greater isolation of the lower water column in  
266 the warmer summer (Figure 6). Near-surface waters were more oxygenated and bottom waters  
267 were more oxygen-depleted in 2012 compared to 2011 (11.7 vs 10.4  $\text{mg L}^{-1}$  at the surface and  
268 2.7 vs 4.7  $\text{mg L}^{-1}$  at the bottom, respectively). During most of summer 2011,  $\text{CO}_2$  levels were  
269 above saturation in surface waters (relative to atmospheric equilibrium), and increased after  
270 rainfall ( $R = 0.6$ ,  $p = 0.04$ ). In contrast, surface waters in 2012 were depleted in  $\text{CO}_2$  between  
271 May and August (by down to  $-5 \mu\text{M}$  below saturation). Diurnal analyses of the  $\text{CO}_2$  saturation  
272 levels in mid-July revealed that even at night,  $\text{CO}_2$  levels at the surface remained low ( $< 2 \mu\text{M}$ ,  
273 Figure S3). This persistent  $\text{CO}_2$  depletion ended after three days of continuous rain in mid-  
274 September, during which the mixed layer deepened (Figure 6 E, F). Consistent with higher  
275 surface water concentrations,  $\text{CO}_2$  fluxes were on average higher in 2011 than in 2012 (8.7  
276 and  $-2.5 \text{ mmol m}^{-2} \text{ d}^{-1}$ ,  $p=0.037$ , Wilcoxon test, Figure 6 G, H). Except for a brief period of high  
277  $\text{CO}_2$  efflux recorded during complete overturn after the summer with heat waves, when  $\text{CO}_2$   
278 emission reached  $78 \text{ mmol m}^{-2} \text{ d}^{-1}$ , the  $\text{CO}_2$  uptake by surface lake waters was more persistent  
279 and higher in 2012 than in 2011, with maximum influx rates of  $-30 \text{ mmol m}^{-2} \text{ d}^{-1}$  during heat  
280 waves in the second half of July.

281

282 The TP and TN concentrations remained high over the entire study period (2011-2012),  
283 indicating eutrophic conditions in the lake. Yet in 2012, summer TP and TN concentrations were  
284 higher than in 2011 (72 vs 45  $\mu\text{g P L}^{-1}$  and 420 vs 370  $\mu\text{g N L}^{-1}$ ). In contrast, concentrations of  
285 inorganic nutrients were lower in surface waters in 2012 than in 2011 (3.5 vs 5.0  $\mu\text{g L}^{-1}$  for SRP,  
286 and 100 vs 150  $\mu\text{g L}^{-1}$  for  $\text{N-NO}_3^-$ ).

287

### 288 **3.4 Phytoplankton**

289 Throughout most of the productive season in 2011, dinophytes dominated the phytoplankton  
290 biomass, starting from June when their biomass reached 96 mg wet weight  $\text{L}^{-1}$  (mg WW  $\text{L}^{-1}$ ;  
291 Figure 7 A, C), corresponding to 15  $\mu\text{g Chl-a L}^{-1}$  (data not shown). In the second half of June,  
292 the total phytoplankton biomass decreased to 30 mg WW  $\text{L}^{-1}$  and consisted of a mixture of  
293 dinophytes, cyanophytes and diatoms. Later that year, diatoms became increasingly abundant  
294 showing a maximum of 401 mg WW  $\text{L}^{-1}$  in the first week of September (Figure 7 A, C).

295

296 Seasonal patterns in phytoplankton biomass were different in 2012 (Figure 7 B). The  
297 phytoplankton was dominated by cryptophytes and diatoms early in the season (May), and  
298 dinophytes in May and June, with the total phytoplankton biomass reaching a maximum of 125  
299 mg WW  $\text{L}^{-1}$ . Buoyant cyanobacteria (*Dolichospermum* sp. and *Aphanizomenon* sp.) were first  
300 evident around 5 July and dominated the phytoplankton community between 20 July and 15  
301 August when they formed a dense surface bloom ( $> 20 \times 10^3$  cells  $\text{ml}^{-1}$  or up to 300 mg WW  
302  $\text{L}^{-1}$ ). Results of the partial least square regression analysis (PLS) revealed that cyanobacterial  
303 biomass can be predicted ( $R^2 = 0.70$ ,  $n = 30$ ,  $p=0.0001$ ) using stratification strength (difference  
304 between surface and bottom T; Variable Importance in the Projection, VIP = 1.9), pH values  
305 (VIP = 1.7) as well as interactions between rainfall and pH (VIP = 1.4) and pH and bottom  $\text{O}_2$

306 (VIP= 1.35). Including the interaction between SRP and N-NO<sub>3</sub> improved these predictions by  
307 additional 8% (VIP = 1.4 R<sup>2</sup>=0.78, p = 0.0001).

308

### 309 **3.5 Sedimentary pigment record and historical data**

310 Temperatures and snowfalls observed in the vicinity of Lake St. Agustin during the last fifty  
311 years correlated with sedimentary pigments (Figure 8; p < 0.05, n = 20). For instance, the Chl-*a*  
312 and β-carotene concentration in surface sediments increased proportionally with summer  
313 temperatures (R = 0.71 and R = 0.59, respectively, p = 0.0001). The concentration of zeaxanthin  
314 (a proxy for cyanobacteria in Lake St. Augustin) and of total cyanobacterial pigments (sum of  
315 zeaxanthin, canthaxanthin and echinenone) were also correlated with summer temperatures (R =  
316 0.78, and 0.69, respectively, p < 0.0001). Noteworthy, canthaxanthin alone showed a negative  
317 relationship to temperatures (R = -0.41, p = 0.1). Decreasing snowfall also influenced  
318 phytoplankton biomass and community structure, as indicated by increase in Chl-*a*, β-carotene  
319 and zeaxanthin concentrations over the last two decades. In contrast to climatic parameters, the  
320 historical TP concentrations (1967-2010; Figure 9) did not correlate with changes in Chl-*a*, β-  
321 carotene or zeaxanthin (n = 14, p > 0.3).

322

323 Changes in zeaxanthin were not linear over time. Consistent with the climate trend  
324 analysis, a sequential t-test followed by an ANOVA showed significant differences with regards  
325 to trends in the concentration of these pigments before and after 1990 (p < 0.001; Figure 9).  
326 Zeaxanthin decreased between 1965 and 1990, and subsequently showed a positive trend  
327 between 1990 and 2011. The historical TP dataset did not reveal any trends over the past 50  
328 years (p > 0.7). In contrast to historical TP concentrations, past pH values and CO<sub>2</sub>  
329 concentrations in surface waters indicate an alkalinization (from an average of pH = 8.3 between

330 1968 and 1998 to pH = 8.8 between 1998 and 2010) and the associated decrease of summertime  
331 CO<sub>2</sub> concentrations (from 25.5 ± 11.9 μM between 1968 and 1998 to 9.3 ± 6.7 μM between 1998  
332 and 2010; R = -0.58, n=12 p=0.02, Figure 9). Historical surface water CO<sub>2</sub> concentrations  
333 correlated to air temperatures recorded over the lake (R = -0.78, p=0.003), and because the  
334 temperature record is more complete, the latter dataset was used in all subsequent analyses.

335

336 The multiple polynomial regression model, considering both climatic parameters (T,  
337 precipitation) and phosphorus concentrations, indicates that most of the variability in  
338 sedimentary zeaxanthin ( $R^2 = 0.75$ , n= 18, p=0.001) can be explained by changes in summer and  
339 winter air temperatures, with an improvement by 15% after including the historical TP data.  
340 Overall, the accumulation of zeaxanthin in the sediments of Lac Saint Augustin, can be well  
341 predicted ( $R^2 = 0.9$ , n=14 p = 0.001) using these three variables. The accumulation of  
342 cyanobacterial pigments can also be predicted using polynomial regression based on climate  
343 characteristics only ( $R^2 = 0.78$ , p=0.001). Including historical TP concentrations results in further  
344 improvement of the model prediction by 10% ( $R^2=0.88$ , p=0.001, n=14).

345

#### 346 **4 DISCUSSION**

347 Effects of meteorological forcing on cyanobacteria in the lake were either direct through  
348 increased surface temperatures (Johnk et al., 2007), or indirect through the modulating control on  
349 the duration and strength of water column stratification, residence time, pH and nutrients.

350 Particularly an interactive effect of enhanced stratification and increasing pH (associated to  
351 lower CO<sub>2</sub> levels) appears as an important catalyzer of cyanobacterial blooms. Our data indicate  
352 that heat waves and long-term warming affect functioning of polymictic lake ecosystem along  
353 the same axis. Correlative analyses of the sedimentary pigment record, historical TP and pH

354 (CO<sub>2</sub> concentrations), and associated meteorological time series, as well as results from a natural  
355 experiment comparing years with contrasting meteorology indicate that warming and pH control  
356 the abundance of buoyant cyanobacteria. On the other hand, our work does not provide support  
357 for the existence of any specific P concentration threshold that may act to trigger blooms of  
358 cyanobacteria, suggesting that nutrients were sufficient already five decades ago to support  
359 persistent summertime blooms. While our results, show that effects of temperature are  
360 interacting with those of alkalinity (CO<sub>2</sub> depletion) when nighttime winds are low and  
361 stratification is strong (Visser et al., 2016) to stimulate cyanobacteria, high frequency monitoring  
362 of hydrodynamics and phytoplankton (Marcé et al., 2016) coupled to models (e.g., Recknagel et  
363 al., 2013) may help to gain further insight into the mechanism of bloom formation.

364

#### 365 **4.1 Warming-related effects on the water column physicochemistry**

366 Heat waves had a strong effect on the stratification of Lake St. Augustin. The surface was  
367 warmer and the bottom colder in 2012 than in 2011. The enhanced temperature gradient during  
368 heat waves impeded exchanges between the upper and lower water column as shown also in  
369 other lakes (Shatwell et al., 2016). The detailed data in Lake St. Augustin indicate how the  
370 mixing dynamics changed during heat waves such that conditions favored cyanobacteria. During  
371 typical weather conditions, winds are moderate over the lake, with maxima between 4 m s<sup>-1</sup> and 6  
372 m s<sup>-1</sup>.  $L_N$  drops below 1, implying the thermocline up and downwells and mixing occurs on a  
373 daily basis (Yeates & Imberger, 2003). On nights when winds remained high, heat losses were  
374 elevated up to -500 W m<sup>-2</sup> and stratification was reduced, as expected with classic polymixis.  
375 During heat waves, winds and  $L_N$  were lower in the day (between 1 and 5), and fetch was  
376 reduced as winds were across rather than along the lake. Thus, while thermocline still tilted, the

377 magnitude of this movement was less, and reduced downward mixing of heat contributed to  
378 greater and more persistent stratification (buoyancy frequencies increased above 40 cph).

379

380 Although air temperatures increased during heat waves, the co-varying decrease in wind  
381 speeds and associated reduction in latent heat fluxes, the major heat loss term for the lake, were  
382 the critical determinants of warming and stratification. In fact, the incoming heat from sensible  
383 heat during heat waves was small ( $<20 \text{ W m}^{-2}$  as compared to between  $-40 \text{ W m}^{-2}$  and  $-100 \text{ W}$   
384  $\text{m}^{-2}$  during windier conditions). With decreased heat losses at night under low winds, more of the  
385 heat which accumulated in the day was retained contributing to more stable stratification.

386

387 Enhanced stratification associated with heat waves resulted in the deoxygenation of bottom  
388 waters. The lake has accumulated large quantities of P in its sediments over the last 50 years, and  
389 currently experiences release of this legacy P when oxygen is depleted (Galvez-Cloutier et al.,  
390 2012). However, because of the ineffective exchange between the bottom and surface (euphotic)  
391 layers of the lake during the summer 2012, this surplus bioavailable P likely remained in the  
392 lower water column where it was accessible for migrating phytoplankton i.e., buoyant  
393 cyanobacteria, but not for other species.

394

395 While alkalinity and  $\text{CO}_2$  levels appear to play an important role in shaping the  
396 phytoplankton community structure (Maileht et al., 2013), their effect may be particularly  
397 important in controlling cyanobacteria (Dam et al., 2018). In the near future many lakes around  
398 the globe will stratify more strongly (Woolway and Merchant 2019) and, with their sediments  
399 remaining colder throughout the summer (Bartosiewicz et al., 2019), less carbon will be release  
400 into the upper layers of the water column. These conditions are likely to favor bloom-forming

401 cyanobacteria (Marcus et al 1983) in the thinner and warmer epilimnion. The persistent diurnal  
402 CO<sub>2</sub> depletion, increasing alkalinity as well as very high rates of CO<sub>2</sub> uptake during the bloom  
403 indicate that buoyant cyanobacteria benefitted from their ability to concentrate carbon around  
404 their cells and migrated to optimize usage of atmospheric CO<sub>2</sub>. In fact, measured CO<sub>2</sub> uptake  
405 rates were higher than expected from estimated values of the gas transfer coefficient (MacIntyre  
406 e al., 2010, Tedford et al., 2013, data not shown,) thus further supporting biologically enhanced  
407 CO<sub>2</sub> influx. Some previous experimental work suggested that cyanobacteria may outcompete  
408 other phytoplankton if CO<sub>2</sub> availability is low and alkalinity high (Caraco & Miller 1998). Our  
409 results (using data from both natural experiment that compared two years and historical records  
410 that spanned over the last five decades) provide observational support for this positive  
411 interaction.

412

413 Here we argue that, in addition to exploiting of bicarbonates and using a highly effective C  
414 concentrating mechanism buoyant cyanobacteria gain an ecological advantage when heatwave-  
415 enhanced stratification allows them to more readily use atmospheric CO<sub>2</sub>. Shallow polymictic  
416 lakes have traditionally been assumed to mix on a daily to weekly basis so that filamentous  
417 cyanobacteria could not use their buoyancy regulation to gain much of an advantage. Yet, here  
418 we demonstrate that during heat waves, and more frequently under future climate, lakes that  
419 mixed often will mix less and become a better habitat for buoyant cyanobacteria.

420

#### 421 **4.2 Decadal warming effects on the phytoplankton community**

422 Historical records provide additional evidence for the link between climate change and  
423 cyanobacterial blooms than our two-year limnological study. The 38% increase in zeaxanthin  
424 between 1990 and 2012 (and in total cyanobacterial pigments), relative to the long-term average,

425 indicates potential recent proliferation of cyanobacteria. This increase coincides with accelerated  
426 warming, increasing pH and decreasing summertime CO<sub>2</sub> levels. The regression analyses reveal  
427 that while the climate variables have high explanatory power in relation to cyanobacterial  
428 pigments, the P concentrations were comparatively less useful in that regard for this eutrophic  
429 lake. The counterintuitive decrease in the sedimentary canthaxanthin may have been associated  
430 to lower contribution from this pigment in the total produced carotenoids under moderate levels  
431 of warming (Halfen & Francis 1972, Klodawska et al., 2019). The potential effects and  
432 interaction of ambient temperature and related environmental conditions (alkalinity) on cell-  
433 specific pigment production in cyanobacteria require further study.

434

435         Our results differ from previous findings indicating that nutrients rather than temperature  
436 control cyanobacterial blooms in lakes (Rigosi et al., 2014). Although we have studied only one  
437 specific lake, we propose that for lakes with a history of high nutrient loading and the efficient  
438 recycling of nutrients (Kilham & Kilham, 1990), continued nutrient input is not a key  
439 determinant of the frequency of harmful cyanobacterial blooms. In fact, many of the earlier  
440 observations pointing towards nutrient supply as the key determinant of cyanobacterial blooms  
441 are from lakes deeper than 10 m that develop blooms once stably stratified. Our data imply that  
442 these results are not necessarily pertinent to polymictic lakes with continuously high nutrient  
443 supply and support previous observations (Kosten et al., 2012) with a more mechanistic  
444 explanation. On the other hand, many shallow lakes host abundant macrophytes that may, under  
445 specific conditions, suppress cyanobacteria (Chang et al., 2012). The impact of climate change  
446 on macrophytes (Li et al., 2017) as well as the impact of macrophytes on water column

447 stratification under warming (Vilas et al., 2017) and thus on the competitive abilities of buoyant  
448 cyanobacteria also requires further investigation.

449

### 450 **4.3 Conclusion**

451 Our results suggest that the synergy between warming and water column stratification is  
452 the key factor catalyzing cyanobacterial blooms in eutrophic polymictic lake. The effects of  
453 meteorological forcing on cyanobacteria blooms are both direct and indirect as they moderate  
454 temperature and precipitation as well as the related duration and strength of stratification. While  
455 persistent stratification and phytoplankton activity leads to elevated pH and enables CO<sub>2</sub> to  
456 remain undersaturated such that cyanobacteria had an advantage over other phytoplankton, our  
457 data imply that this effect can trigger cyanobacterial blooms only when acting in combination  
458 with lower nighttime winds and concomitant rapid warming of surface waters. Blooms of  
459 buoyant cyanobacteria will occur more frequently in polymictic lakes as climate warms and as  
460 these waters stratify more strongly. Harmful phytoplankton blooms under such conditions will  
461 have profound consequences for the biogeochemistry and aquatic food webs and hence for the  
462 functioning of aquatic ecosystems.

463 **Acknowledgements**

464 This project was funded from a NSERC Discovery grant to IL. SM and AC were funded from  
465 U.S. NSF Arctic Natural Sciences (ARC) Grants #120426 and #1737411 to SM. During the  
466 preparation of this manuscript, MB and AP were supported from Basel University Research  
467 Funds and SNF grant to MFL and MB.

468

469 **REFERENCES**

- 470 Bartosiewicz, M., Laurion, I., & MacIntyre, S. (2015). Greenhouse gas emission and storage in a  
471 small shallow lake. *Hydrobiologia*, 757, 101–115. DOI: 10.1007/s10750-015-2240-2
- 472 Bartosiewicz, M., Laurion, I., Clayer, F., & Maranger, R. (2016). Heat-wave effects on oxygen,  
473 nutrients, and phytoplankton can alter global warming potential of gases emitted from a small  
474 shallow lake. *Environmental Science & Technology*, 50, 6267–6275. DOI:  
475 10.1021/acs.est.5b06312.
- 476 Bartosiewicz, M., Przytulska, A., Lapierre, J.F., Laurion, I., Lehmann, M.F. & Maranger, R. Hot  
477 tops, cold bottoms: Synergistic climate warming and shielding effects increase carbon burial  
478 in lakes. *Limnology and Oceanography Letters*, 00–000.
- 479 Bergeron, M., Corbeil, C., & Arsenault, S. (2002). Diagnose écologique du lac Saint Augustin.  
480 EXXEP Environnement, Québec, 70 pp.
- 481 Caraco, N. F., & Miller, R. (1998). Effects of CO<sub>2</sub> on competition between a cyanobacterium  
482 and eukaryotic phytoplankton. *Canadian Journal of Fisheries and Aquatic Sciences*, 55, 54–  
483 62.
- 484 Chang, X., Eigemann, F., & Hilt, S. (2012). Do macrophytes support harmful cyanobacteria?  
485 Interactions with a green alga reverse the inhibiting effects of macrophyte allelochemicals on  
486 *Microcystis aeruginosa*. *Harmful Algae*, 19, 76-84.
- 487 Chen C. T., & Millero F. J. (1977). Speed of sound in seawater at high pressures. *The Journal of*  
488 *the Acoustical Society of America*, 62, 1129–1135. doi: 10.1121/1.381646
- 489 de Senerpont Domis L. N., Mooij W. M., & Huisman J. (2007). Climate-induced shifts in an  
490 experimental phytoplankton community: a mechanistic approach. *Hydrobiologia*, 584, 403–  
491 413. DOI: 10.1007/s10750-007-0609-6
- 492 Deshpande, B. N., Tremblay, R., Pienitz, R., & Vincent, W. F. (2014). Sedimentary pigments as  
493 indicators of cyanobacterial dynamics in a hypereutrophic lake. *Journal of Paleolimnology*,  
494 52, 171–184. DOI: 10.1007/s10933-014-9785-3
- 495 Dibike, Y., Prowse, T., Saloranta, T., & Ahmed, R. (2011). Response of Northern Hemisphere  
496 lake-ice cover and lake-water thermal structure patterns to a changing climate. *Hydrological*  
497 *Processes*, 25, 2942–2953. <https://doi.org/10.1002/hyp.8068>

498 Galvez-Cloutier, R., Saminathan, S. K., Boillot, C., Triffaut-Bouchet, G., Bourget, A., &  
499 Soumis-Dugas, G. (2012). An evaluation of several in-lake restoration techniques to improve  
500 the water quality problem (eutrophication) of St.-Augustin Lake, Quebec, Canada.  
501 *Environmental management*, 49, 1037–1053. DOI: 10.1007/s00267-012-9840-7

502 Ganf G. C., & Oliver R. L. (1982). Vertical separation of light and available nutrients as a factor  
503 causing replacement of green algae by blue-green algae in the plankton of a stratified lake.  
504 *Journal of Ecology*, 70, 829–844. DOI: 10.2307/2260107

505 Gobler, C. J., Burkholder, J. M., Davis, T. W., Harke, M. J., Stow, C. A., & van de Waal, D. B.  
506 (2016). The dual role of nitrogen supply in controlling the growth and toxicity of  
507 cyanobacterial blooms. *Harmful Algae*, 54, 87–97. DOI: 10.1016/j.hal.2016.01.010

508 Halfen, L. N., & Francis, G. W. (1972). The influence of culture temperature on the carotenoid  
509 composition of the blue-green alga, *Anacystis nidulans*. *Archives of Microbiology*, 81, 25–35.

510 Havens, K., Paerl, H., Phlips, E., Zhu, M., Beaver, J. & Srifa, A. (2016). Extreme weather events  
511 and climate variability provide a lens to how shallow lakes may respond to climate change.  
512 *Water*, 8, 229. DOI: 10.3390/w8060229

513 Hillebrand H., Durselen C. D. D., Kirschtel U., Pollinger T., & Zohary T. (1999). Biovolume  
514 calculation for pelagic and benthic microalgae. *Journal of Phycology*, 35, 403–424. DOI:  
515 10.1046/j.1529-8817.1999.3520403.x

516 Ho J.C. & Michalak A. M. (2015). Challenges in tracking harmful algal blooms: a synthesis of  
517 evidence from Lake Erie. *Journal of Great Lakes Research*, 35, 317–325. DOI:  
518 10.1016/j.jglr.2015.01.001

519 Huber V., Wagner C., Gerten D. & Adrian R. (2012). To bloom or not to bloom: contrasting  
520 responses of cyanobacteria to recent heat waves explained by critical thresholds of abiotic  
521 drivers. *Oecologia*, 169, 245–256. DOI: 10.1007/s00442-011-2186-7

522 Ibelings B. W. & Maberly S. C. (1998). Photoinhibition and the availability of inorganic carbon  
523 restrict photosynthesis by surface blooms of cyanobacteria. *Limnology and Oceanography*,  
524 43, 408–419. DOI: 10.4319/lo.1998.43.3.0408

525 Imberger J. (1985). The diurnal mixed layer. *Limnology & Oceanography*, 30, 737–770. DOI:  
526 10.4319/lo.1985.30.4.0737

527 Imberger J. & Patterson J.C. (1990). Physical limnology *Advances in applied mechanics*, 27,  
528 303–475.

529 Jankowski, T., Livingstone, D. M., Bühner, H., Forster, R., & Niederhauser, P. (2006).  
530 Consequences of the 2003 European heat wave for lake temperature profiles, thermal  
531 stability, and hypolimnetic oxygen depletion: Implications for a warmer world. *Limnology  
532 and Oceanography*, 51, 815–819. DOI: 10.4319/lo.2006.51.2.0815

533 Johnk, K. D., Huisman, J. E. F., Sharples, J., Sommeijer, B. E. N., Visser, P. M., & Stroom, J. M.  
534 (2008). Summer heatwaves promote blooms of harmful cyanobacteria. *Global Change  
535 Biology*, 14, 495–512. DOI: 10.1111/j.1365-2486.2007.01510.x

536 Karl T. R., & Trenberth K. E. (2003). Modern global climate change. *Science*, 302, 1719. DOI:  
537 10.1126/science.1090228

538 Karnauskas, K. B., J. K. Lundquist, & L. Zhang. 2018. Southward shift of the global wind  
539 energy resource under high carbon dioxide emissions. *Nature Geoscience*, 11, 38–43. DOI:  
540 10.1038/s41561-017-0029-9

541 Kilham, P. & Kilham, S. (1990). Endless summer: Internal loading processes dominate nutrient  
542 cycling in tropical lakes. *Freshwater Biology*, 23, 379–389. DOI: /10.1111/FWB.1990.23

543 Kłodawska, K., Bujas, A., Tuross-Cabal, M., Żbik, P., Fu, P., & Malec, P. (2019). Effect of  
544 growth temperature on biosynthesis and accumulation of carotenoids in cyanobacterium  
545 *Anabaena* sp. PCC 7120 under diazotrophic conditions. *Microbiological Research*, 226, 34–  
546 40.

547 Kosten, S., Huszar, V. L., Bécares, E., Costa, L. S., Donk, E., Hansson, L. A., & Meester, L.  
548 (2012). Warmer climates boost cyanobacterial dominance in shallow lakes. *Global Change  
549 Biology*, 18, 118–126. DOI: 10.1111/j.1365-2486.2011.02488.x

550 Kraemer, B. M., Mehner, T., & Adrian, R. (2017). Reconciling the opposing effects of warming  
551 on phytoplankton biomass in 188 large lakes. *Scientific reports*, 7(1), 10762. DOI:  
552 10.1038/s41598-017-11167-3.

553 Laurion, I., Vincent, W. F., MacIntyre, S., Retamal, L., Dupont, C., Francus, P., & Pienitz, R.  
554 (2010). Variability in greenhouse gas emissions from permafrost thaw ponds. *Limnology and  
555 Oceanography*, 55, 115–133. DOI: 10.4319/lo.2010.55.1.0115.

556 Li, Z.Q., He, L., Zhang, H., Urrutia-Cordero, P., Ekvall, M.K., Hollander, J., et al., 2017.  
557 Climate warming and heat waves affect reproductive strategies and interactions between  
558 submerged macrophytes. *Glob. Chang. Biol.* 23 (1), 108–116.

559 MacIntyre S., Romero J. R., & Kling G. W. (2002). Spatial-temporal variability in surface layer  
560 deepening and lateral advection in an embayment of Lake Victoria, East Africa. *Limnology  
561 and Oceanography*, 47, 656–671. DOI: 10.4319/lo.2002.47.3.0656

562 MacIntyre S., Fram J. P., Kushner P. J., Bettez N. D., O'Brien W. J., Hobbie J. E., & Kling, G.W.  
563 (2009). Climate-related variations in mixing dynamics in an Alaskan arctic lake. *Limnology  
564 and Oceanography*, 54, 2401–2417. DOI: 10.4319/lo.2009.54.6/

565 MacIntyre, S., A. Jonsson, M. Jansson, J. Aberg, D. E. Turney & S. D. Miller, 2010. Buoyancy  
566 flux, turbulence, and the gas transfer coefficient in a stratified lake. *Geophysical Research  
567 Letters* 37: L24604.

568 MacIntyre, S., Crowe, A. T., Cortés, A., & Arneborg, L. (2018). Turbulence in a small arctic  
569 pond. *Limnology and Oceanography*, 00-000. DOI: 10.1002/lno.10941

570 Maileht, K., Nöges, T., Nöges, P., Ott, I., Mischke, U., Carvalho, L., & Dudley, B. (2013).  
571 Water colour, phosphorus and alkalinity are the major determinants of the dominant  
572 phytoplankton species in European lakes. *Hydrobiologia*, 704, 115–126. DOI: 10.1007/s10750-  
573 012-1348-x.

574 Marcé, R., George, G., Buscarinu, P., Deidda, M., Dunalska, J., de Eyto, E., ... & Moreno-Ostos,  
575 E. (2016). Automatic high frequency monitoring for improved lake and reservoir  
576 management. *Environmental Science & Technology*, 50, 10780–10794.

577 Marcus, Y., Havel, E. and Kaplan, A. (1983). Adaptation of the cyanobacterium *Anabaena*  
578 *variabilis* to low CO<sub>2</sub> concentrations in their environment. *Plant Physiology*, 71, 208–210.  
579 DOI: 0.1104/pp.71.1.208

580 Millero, F. J., Pierrot, D., Lee, K., Wanninkhof, R., Feely, R., Sabine, C. L., Key, R. D. &  
581 Takahashi, T. (2002). Dissociation constants for carbonic acid determined from field  
582 measurements. *Deep Sea Research Part I: Oceanographic Research Papers*, 49, 1705–1723.

583 Paerl H. W., Hall N. S., & Calandrino E.S. (2011). Controlling harmful cyanobacterial blooms in  
584 a world experiencing anthropogenic and climatic-induced change. *Science of the Total  
585 Environment*, 409, 1739–1745. DOI: 10.1016/j.scitotenv.2011.02.001

586 Pawlowicz, R. (2008). Calculating the conductivity of natural waters. *Limnology and  
587 Oceanography: Methods*, 6 (9), 489–501. DOI: 10.4319/lom.2008.6.489

588 Pienitz, R., Roberge, K., & Vincent, W. F. (2006). Three hundred years of human-induced  
589 change in an urban lake: paleolimnological analysis of Lac Saint-Augustin, Quebec City,  
590 Canada. *Botany*, 84, 303–320.

591 Posch T., Köster O., Salcher M. M., & Penthaler J. (2012). Harmful filamentous cyanobacteria  
592 favoured by reduced water turnover with lake warming. *Nature Climate Change*, 2, 809–813.  
593 DOI: 10.1038/nclimate1581

594 Recknagel, F., Ostrovsky, I., Cao, H., Zohary, T., & Zhang, X. (2013). Ecological relationships,  
595 thresholds and time-lags determining phytoplankton community dynamics of Lake Kinneret,  
596 Israel elucidated by evolutionary computation and wavelets. *Ecological Modelling*, 255, 70–  
597 86.

598 Reichwaldt, E. S., & Ghadouani, A. (2012). Effects of rainfall patterns on toxic cyanobacterial  
599 blooms in a changing climate: between simplistic scenarios and complex dynamics. *Water*  
600 *Research*, 46, 1372–1393. DOI: 10.1016/j.watres.2011.11.052

601 Rigosi, A., Carey, C. C., Ibelings, B. W., & Brookes, J. D. (2014). The interaction between  
602 climate warming and eutrophication to promote cyanobacteria is dependent on trophic state  
603 and varies among taxa. *Limnology and Oceanography*, 59, 99–114. DOI:  
604 10.4319/lo.2014.59.1.0099

605 Schlüter, L., Lauridsen, T. L., Krogh, G., & Jørgensen, T. (2006). Identification and  
606 quantification of phytoplankton groups in lakes using new pigment ratios—a comparison  
607 between pigment analysis by HPLC and microscopy. *Freshwater Biology*, 51, 1474–1485.

608 Shatwell, T., Adrian, R., & Kirillin, G. (2016). Planktonic events may cause polymictic-dimictic  
609 regime shifts in temperate lakes. *Scientific reports*, 6. DOI: 10.1038/srep24361

610 Stainton, M. P., Capel, M. J., & Armstrong, F. A. J. (1977). The chemical analysis of freshwater,  
611 2nd ed. Canadian Fisheries and Marine Service Miscellaneous Special Publication 25, 180 pp.

612 Taranu, Z. E., Gregory-Eaves, I., Leavitt, P. R., Bunting, L., Buchaca, T., Catalan, J. &  
613 Moorhouse, H. (2015). Acceleration of cyanobacterial dominance in north  
614 temperate-subarctic lakes during the Anthropocene. *Ecology Letters*, 18, 375–384. DOI:  
615 10.1111/ele.12420.

616 Tedford, E. W., S. MacIntyre, S. D. Miller & M. J. Czikowsky, 2014. Similarity scaling of  
617 turbulence in a temperate lake during fall cooling. *Journal of Geophysical Research*. doi:  
618 10.1002/2014JC010135.

619 Utermöhl, H. (1958). Zur Vervollkommung der quantitativen Phytoplankton-Methodik.  
620 Mitteilungen. *Internationale Vereinigung fuer Theoretische und Angewandte Limnologie*, 9,  
621 1–38.

622 Van Dam, B. R., Tobias, C., Holbach, A., Paerl, H. W., & Zhu, G. (2018). CO<sub>2</sub> limited  
623 conditions favor cyanobacteria in a hypereutrophic lake: An empirical and theoretical stable  
624 isotope study. *Limnology and Oceanography*, 00-000. DOI: 10.1002/lno.10798

625 Verpoorter, C., Kutser, T., Seekell, D. A. & Tranvik, L. J. (2014). A global inventory of lakes  
626 based on high-resolution satellite imagery. *Geophysical Research Letters*, 41, 2014GL060641.

627 Vilas, M. P., C. L. Marti, C. E. Oldham & Hipsey, 2018. Macrophyte-induced thermal  
628 stratification in a shallow urban lake promotes conditions suitable for N-fixing cyanobacteria.  
629 *Hydrobiologia*. <https://doi.org/10.1007/s10750-017-3376-z>.

630 Visser, P. M., Ibelings, B. W., Bormans, M., & Huisman, J. (2016). Artificial mixing to control  
631 cyanobacterial blooms: a review. *Aquatic Ecology*, 50, 423–441. DOI: 10.1007/s10452-015-  
632 9537-0

633 Winterman J. F. G. M., & de Mots A. (1965). Spectrophotometric determination of chlorophylls  
634 a and b and their pheophytins in ethanol. *Biochimica et Biophysica Acta*, 109, 448–453. DOI:  
635 10.1016/0926-6585(65)90170-6

636 Woolway, R. I. and Merchant, C. J. (2019) Worldwide alteration of lake mixing regimes in  
637 response to climate change. *Nature Geoscience*, 12, 271–276.

638 Yeates, P. S., and J. Imberger. 2003. Pseudo two-dimensional simulations of internal and  
639 boundary fluxes in stratified lakes and reservoirs. *International Journal of River Basin*  
640 *Management*, 1, 297–319. DOI: 10.1080/15715124.2003.9635214.

641 Zapata, M., Rodriguez, F., & Garrido, J. L. (2000). Separation of chlorophylls and carotenoids  
642 from marine phytoplankton: A new HPLC method using a reversed phase C8 column and  
643 pyridine-containing mobile phases. *Marine Ecology Progress Series*, 195, 29–45. DOI:  
644 10.3354/meps195029

645 **Table 1.** Wind speed, rainfall and limnological characteristics of Lake St-Augustin during the natural experiment comparing two years  
646 (2011 and 2012). Water temperature (T), dissolved oxygen (O<sub>2</sub>) and total phosphorus (TP) are given both for surface (S) and bottom  
647 waters (B). Nutrients and Chl-a concentrations as well as total phytoplankton abundance (Biomass) were measured in duplicates on ten  
648 sampling dates in 2011 and twenty sampling dates in 2012 (total of 60 values for each parameter); CO<sub>2</sub> concentrations were measured in  
649 triplicates (n= 90).  
650  
651

Var.	Wind	Rain	T <sup>S</sup>	T <sup>B</sup>	O <sub>2</sub> <sup>S</sup>	O <sub>2</sub> <sup>B</sup>	TP <sup>S</sup>	TP <sup>B</sup>	SRP	TN	N-NO <sub>3</sub> <sup>-</sup>	Chl-a	Biomass	pH	CO <sub>2</sub>
Unit	m s <sup>-1</sup>	mm	°C	°C	mg L <sup>-1</sup>	mg L <sup>-1</sup>	µg L <sup>-1</sup>	µg L <sup>-1</sup>	µg L <sup>-1</sup>	µg L <sup>-1</sup>	mg L <sup>-1</sup>	µg L <sup>-1</sup>	mg L <sup>-1</sup>		µmol
2011	3.3	590	17	19	10.4	4.7	45	95	5.0	370	150	14	99	8.4	6.8
2012	3.6	810	21	18	11.7	2.7	72	89	3.5	420	100	21	110	8.6	-0.98

652 **CAPTIONS**

653 **Figure 1.** Bathymetric map of Lake St. Augustin with inset indicating the location of this study  
654 site and black square indicating location of the sampling station on the lake. Thermistor chain  
655 was deployed 10 m inshore from the station where the water column was only 4.5 m deep.

656 **Figure 2.** Regional signatures of climate change including trends in the average, maximum  
657 (winter) and minimum (summer) temperatures, as well as the cumulated annual snowfall and  
658 rainfall over Lake St. Augustin between 1950 and 2010.

659 **Figure 3.** Wind speed spectra (hourly winds in 2011 and at 8 min intervals in 2012), daytime  
660 maximum and nighttime minimum temperatures, as well as daily and total rainfall at Lake St.  
661 Augustin during an average (blue) and a heat-wave year (red). Red arrows indicate heat events,  
662 dotted black line indicates long-term average monthly temperatures.

663 **Figure 4.** Two hourly averaged wind speeds, Lake Numbers and heat fluxes along with  
664 temperature structure in Lake St. Augustin during summer of 2012.

665 **Figure 5.** Hourly averaged wind speeds, Lake Numbers, temperature and buoyancy frequencies  
666 (N) as well as mixed layer depths during the period with heat waves in 2012. Near surface N  
667 exceeded 20 cph on days with heat gain, and on days with greatest heat gain N exceeded 40 cph.

668 **Figure 6.** Seasonal changes in daytime surface and bottom water temperatures, dissolved oxygen  
669 (DO), carbon dioxide departure from saturation levels (CO<sub>2</sub>, triplicate measurements) and fluxes  
670 at the water-atmosphere interface in Lake St. Augustin during 2011 (left panels) and 2012 (right  
671 panels).

672 **Figure 7.** Seasonal changes in the plankton biomass, including phytoplankton (as wet weight)  
673 and zooplankton (as dry weight), as well as the relative contribution of seven main taxonomic  
674 groups to the overall phytoplankton biovolume in Lake St. Augustin during an average wet  
675 (2011, left panels) and hot summer (2012, right panels). Yellow-shaded indicate major heat  
676 events in 2012 (upper panel).

677 **Figure 8.** Correlations between concentrations of selected pigments in the sediments of Lake St.  
678 Augustin and climate indices (average summer and winter temperature, cumulated annual  
679 snowfall).

680 **Figure 9.** Sedimentary pigment profiles (redrawn at higher temporal resolution following  
681 Deshpande et al., 2014), historical meteorological conditions and total phosphorus  
682 concentrations in Lake St. Augustin between 1960 and 2010.

683

684

685

686

687

688 **SUPPLEMENTARY CAPTIONS**

689 **Figure S1.** Changes in monthly average temperatures over Lake St. Augustin winter and summer  
690 months for the period between 1955 and 1990 (white circles) and from 1990 to 2010 (black  
691 circles). The p-values indicate results of an ANCOVA when a significant difference in the slope  
692 or elevation (August) was observed between period 1953-1989 and 1989-2010.

693 **Figure S2.** Preliminary estimation of the coefficient of eddy diffusivity ( $K_z$ ) calculated using the  
694 heat budget method of Jassby and Powell (1975) with the thermistor data Gaussian-filtered for a  
695 3-d period to avoid contamination of the heat budgets by internal wave motions. The heat budget  
696 method is a 1D approach that allows to estimate  $K_z$  only whenever the lake is gaining heat and  
697 lateral advection is minor (MacIntyre, Clark, Jellison, & Fram, 2009a).

698 **Figure S3** Diurnal changes in the CO<sub>2</sub> fluxes at the water-air interface during the cyanobacterial  
699 bloom (July 2012) in lake St-Augustin.

Figure 1

[Click here to download high resolution image](#)

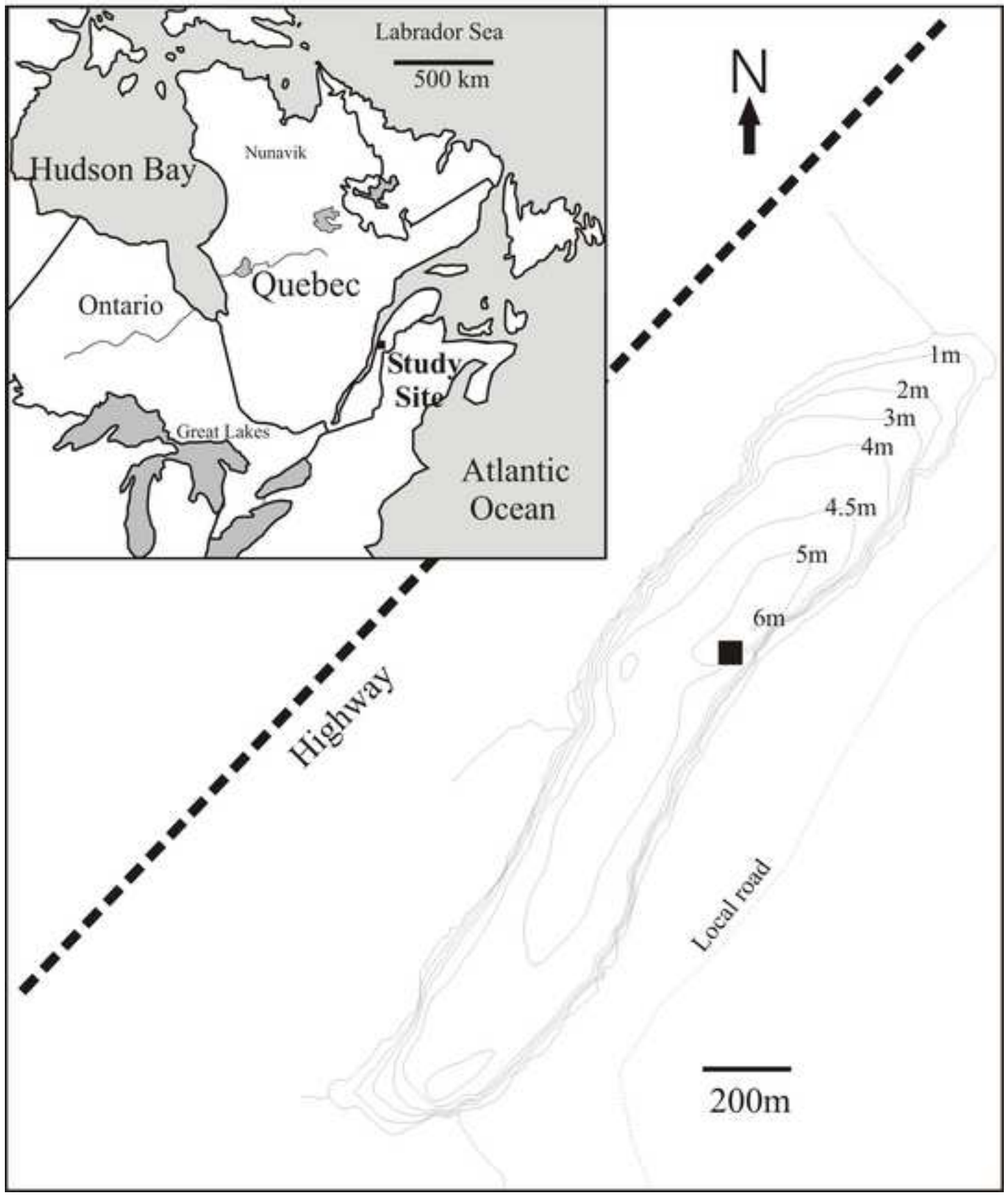


Figure 2  
[Click here to download high resolution image](#)

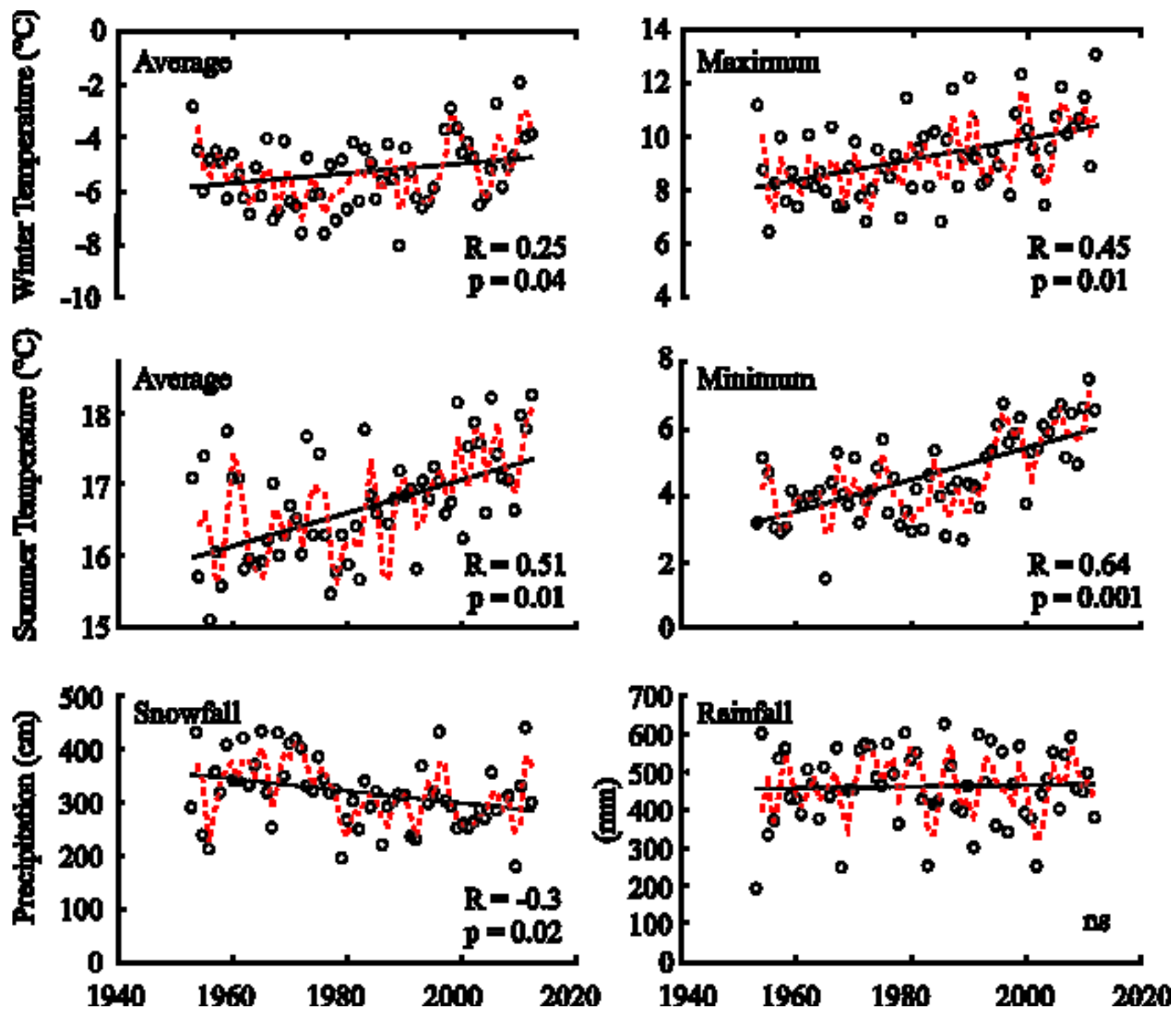


Figure 3  
[Click here to download high resolution image](#)

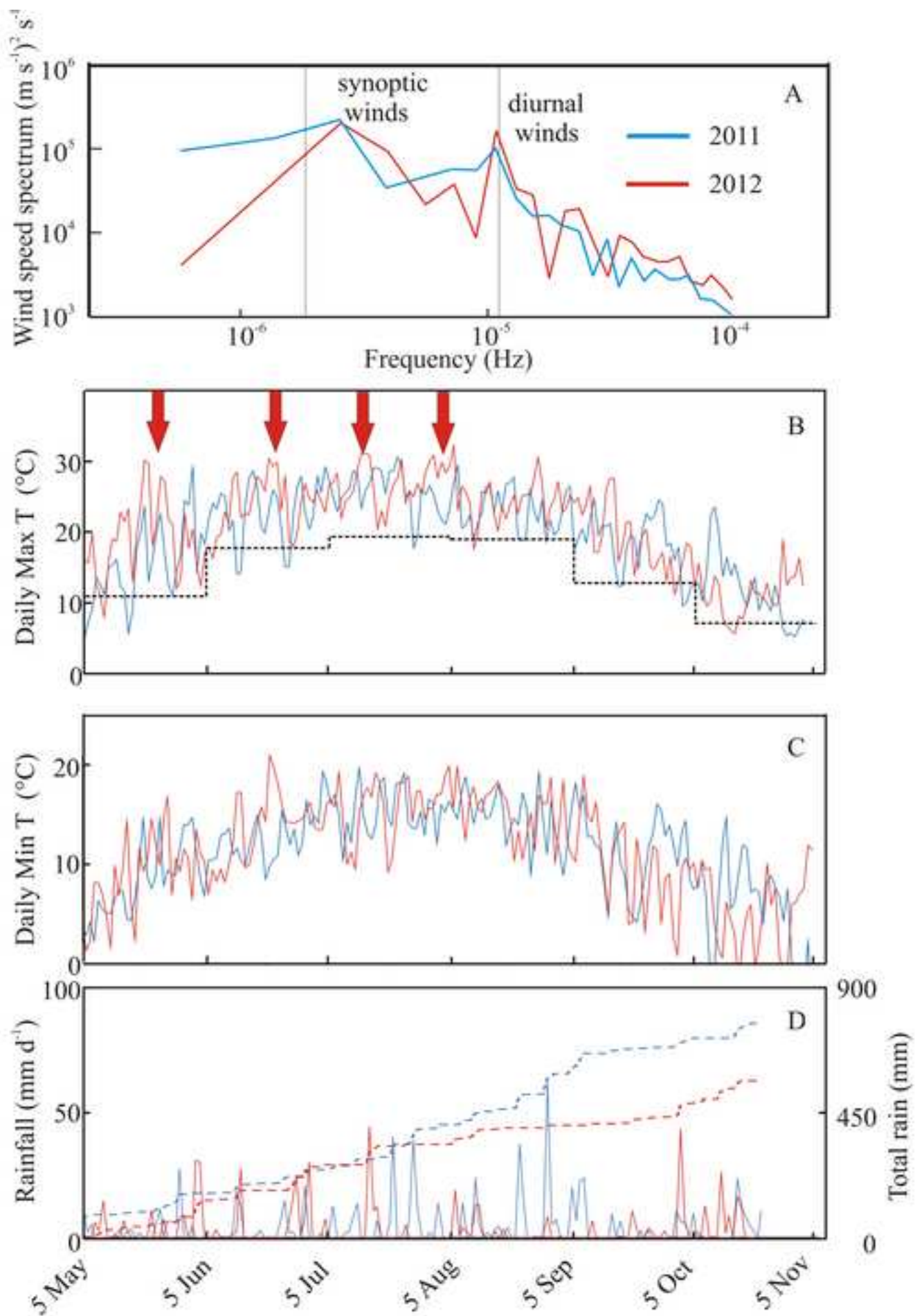


Figure 4  
[Click here to download high resolution image](#)

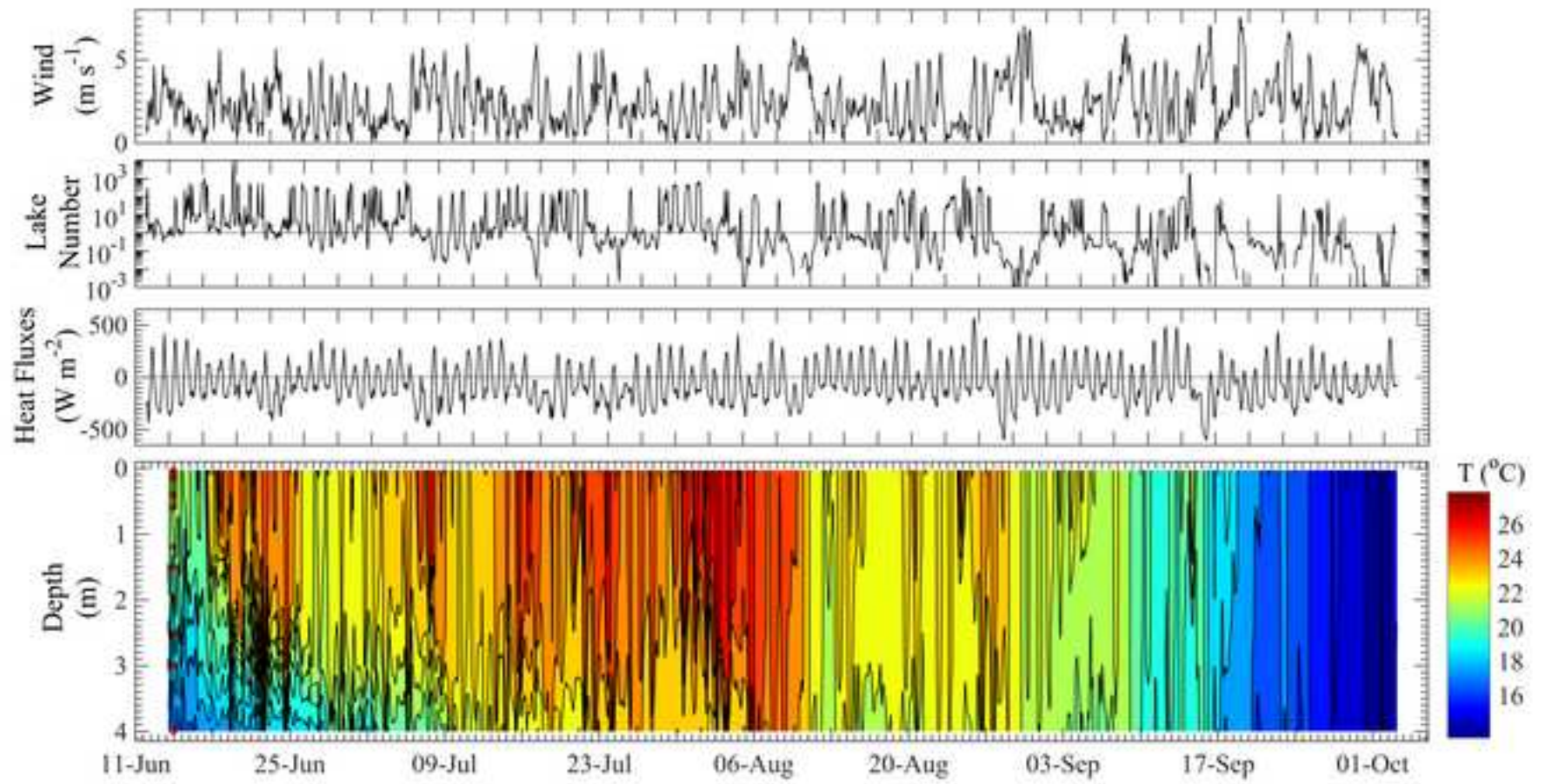


Figure 5  
[Click here to download high resolution image](#)

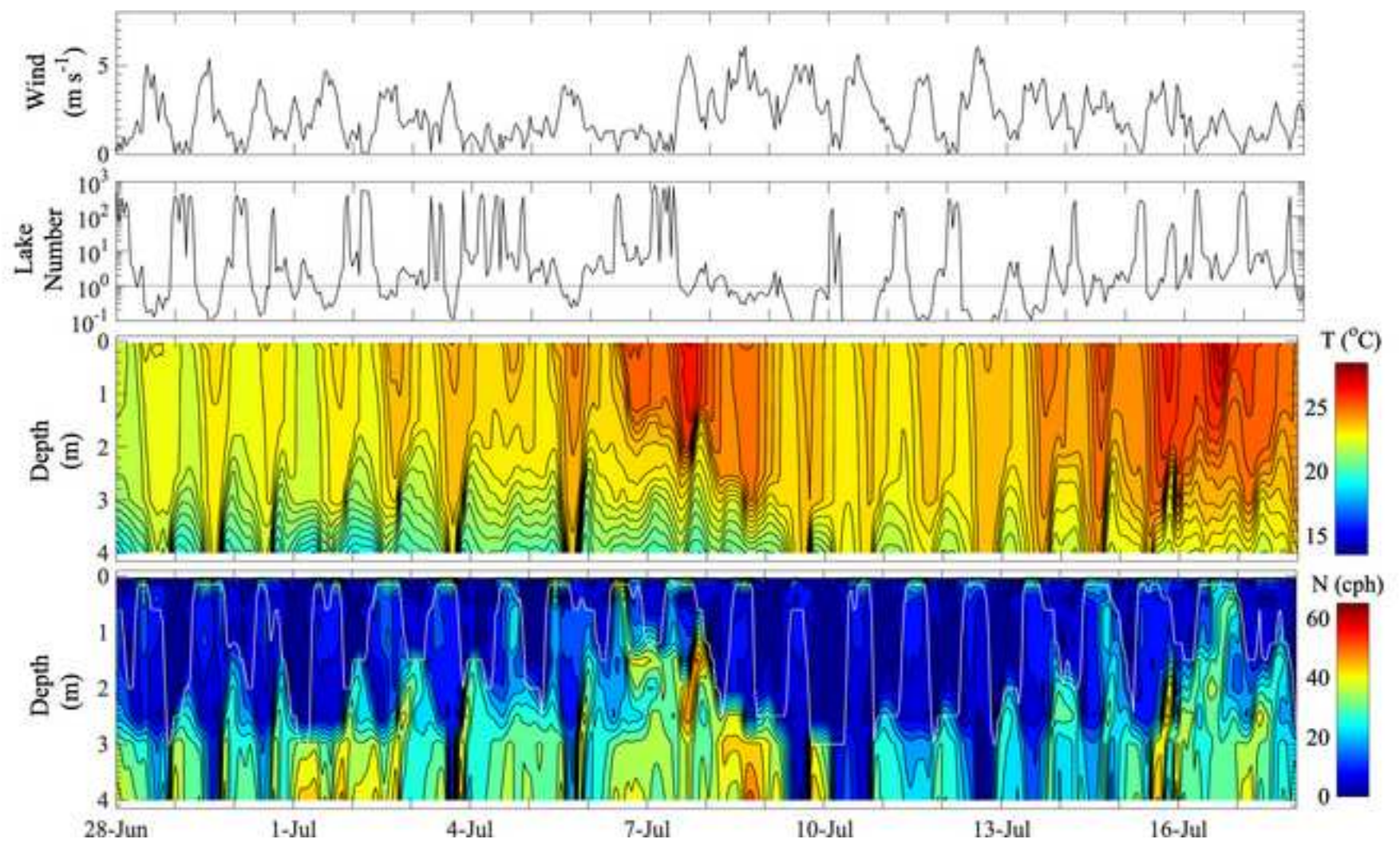


Figure 6  
[Click here to download high resolution image](#)

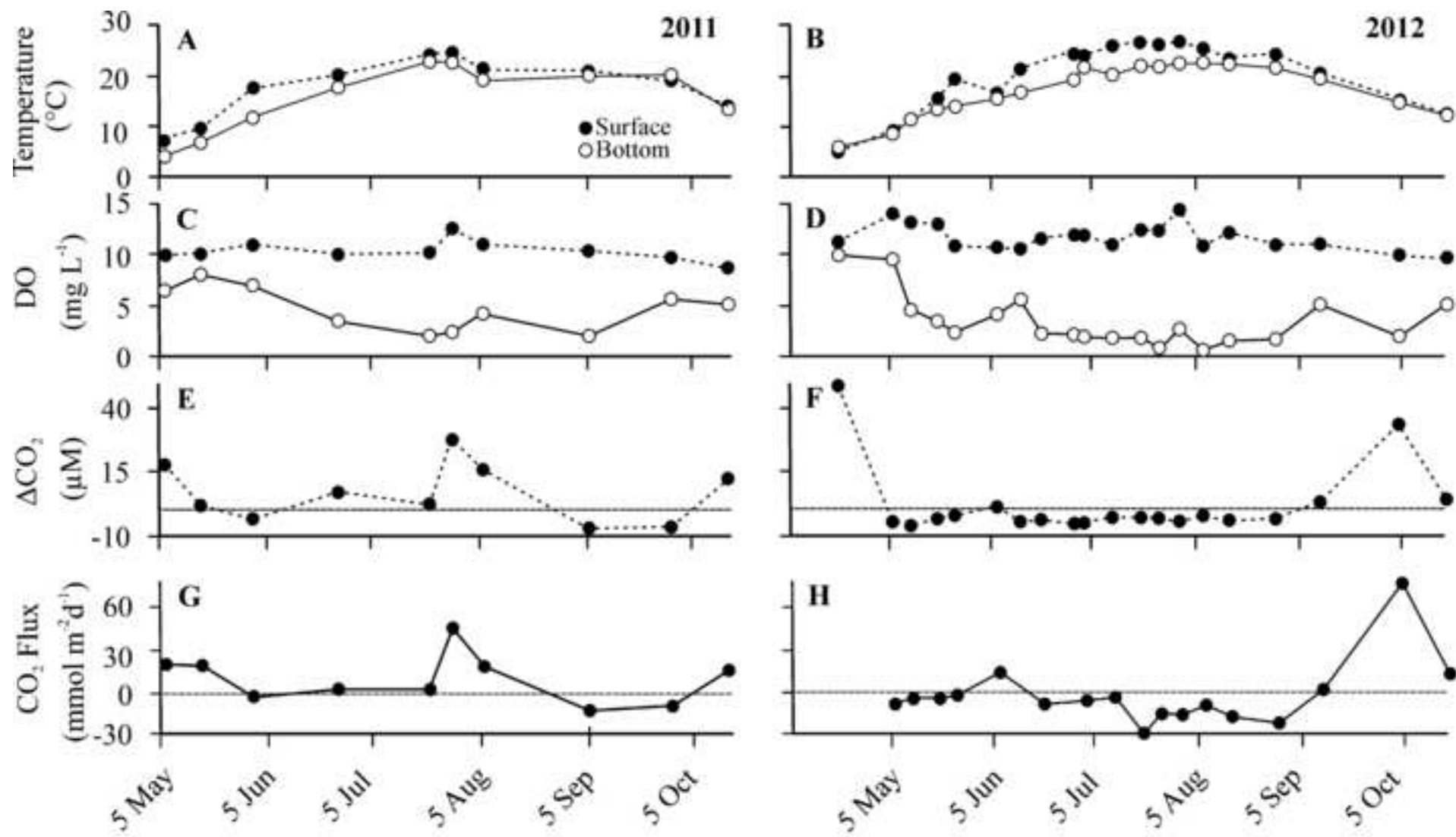


Figure 7  
[Click here to download high resolution image](#)

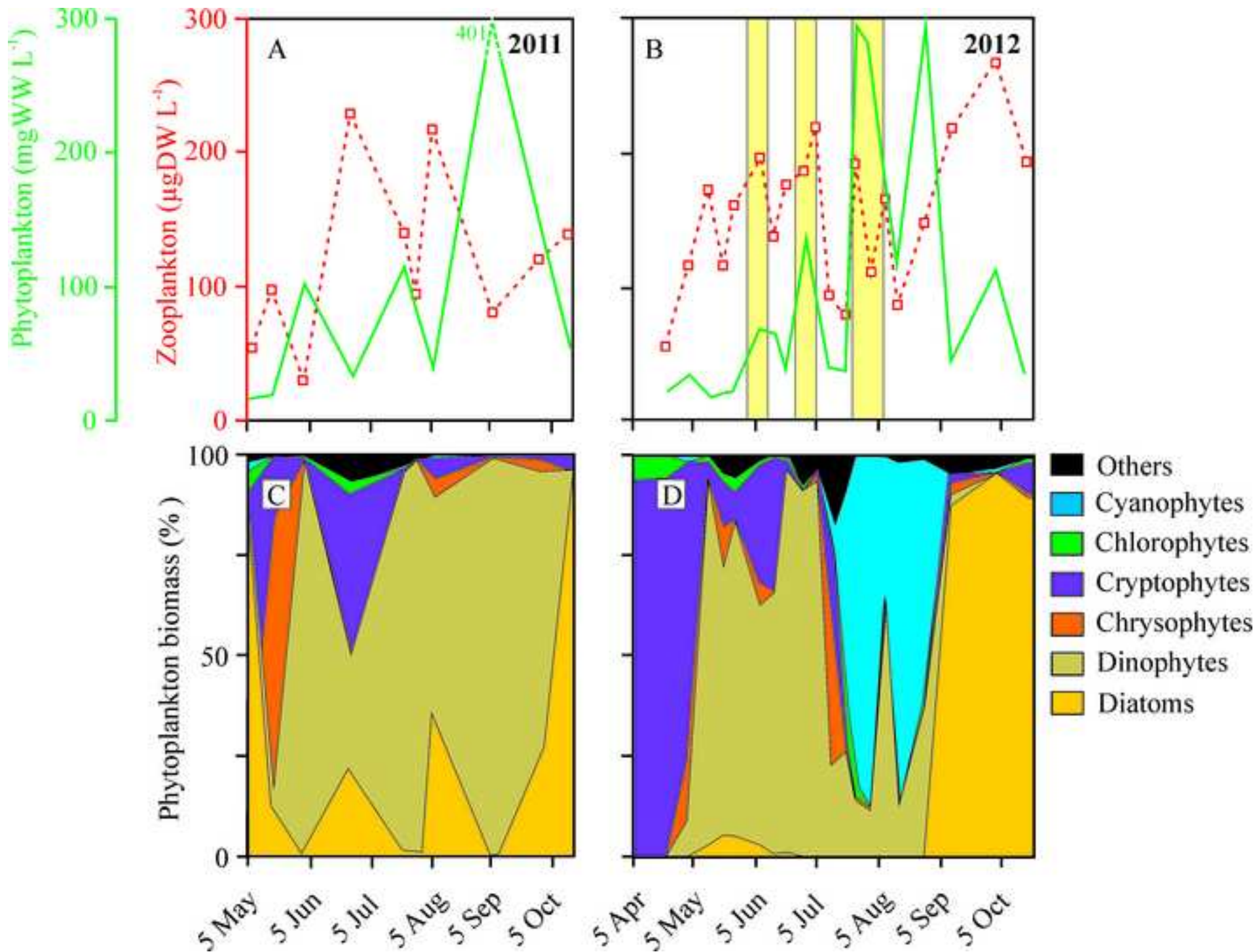


Figure 8  
[Click here to download high resolution image](#)

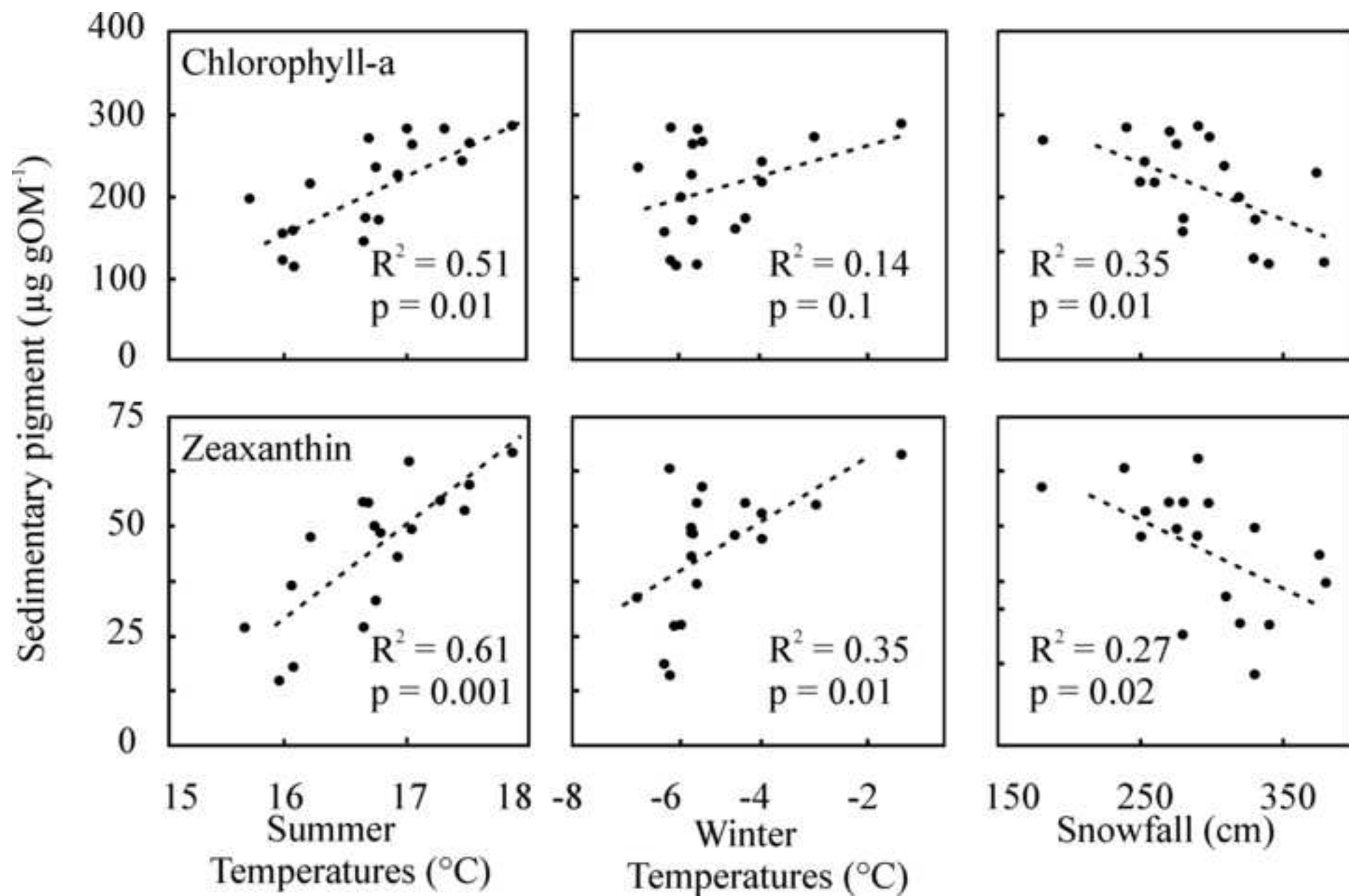
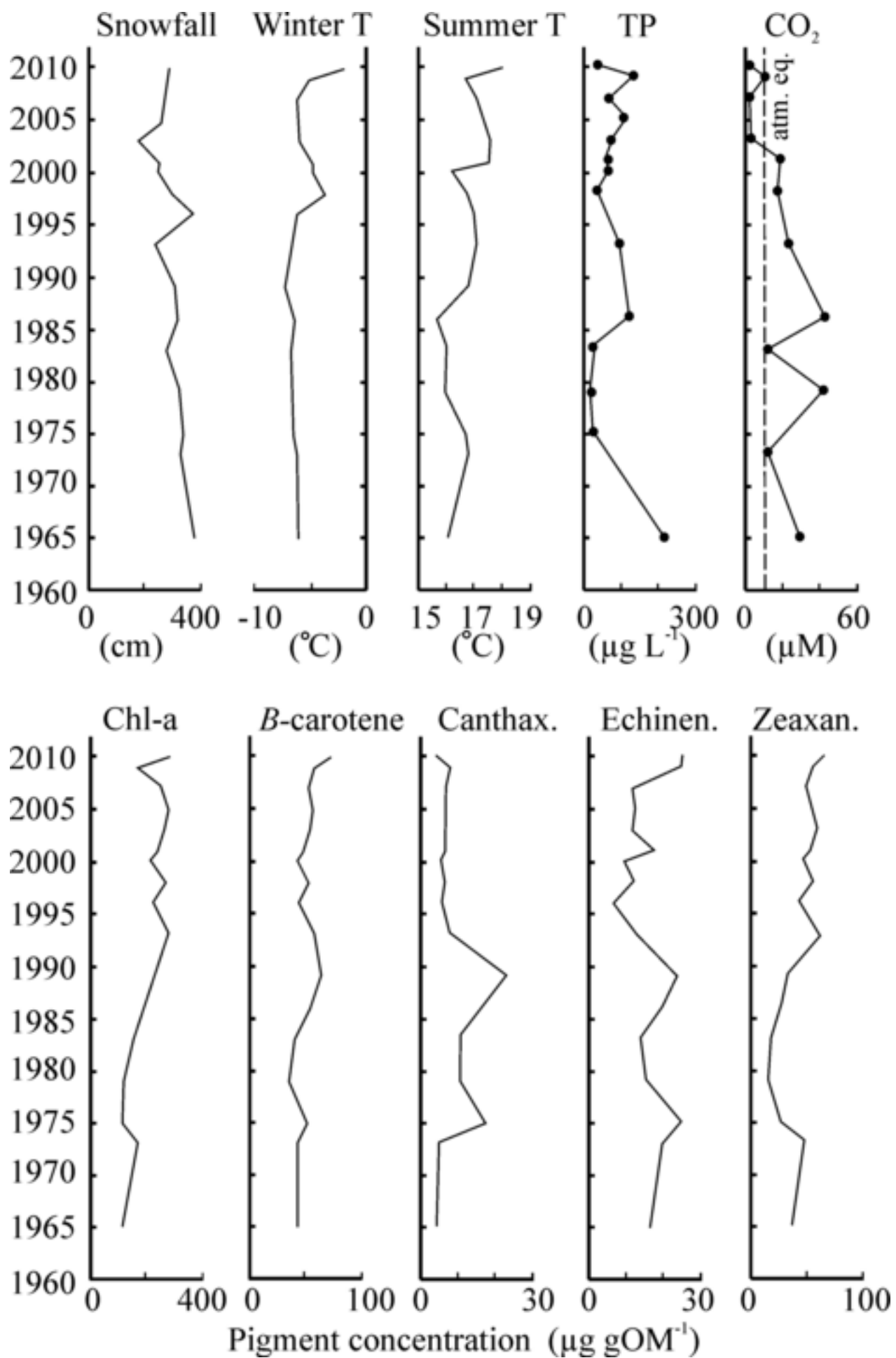


Figure 9

[Click here to download high resolution image](#)



**Fig S1**  
[Click here to download Supplementary material for on-line publication only: Fig S1.TIF](#)

**Fig S2**

[Click here to download Supplementary material for on-line publication only: Figure S2.tif](#)

**Fig S3**

[Click here to download Supplementary material for on-line publication only: Figure S3.tif](#)

**Table S1**  
[Click here to download Supplementary material for on-line publication only: Table S1.docx](#)